Biochimica et Biophysica Acta 1814 (2011) 409–419

Contents lists available at ScienceDirect

Biochimica et Biophysica Acta

journal homepage: www.elsevier.com/locate/bbapap

A novel approach for the purification and proteomic analysis of pathogenic immunoglobulin free light chains from serum

Francesca Lavatelli [a,b], Francesca Brambilla [c], Veronica Valentini [a], Paola Rognoni [a], Simona Casarini [a], Dario Di Silvestre [c], Vittorio Perfetti [d], Giovanni Palladini [a,e], Gabriele Sarais [f], Pierluigi Mauri [c], Giampaolo Merlini [a,e,f,*]

[a] Centro per lo Studio e la Cura delle Amiloidosi Sistemiche, Fondazione IRCCS Policlinico San Matteo, Pavia, Italy
[b] Department of Bioengineering and Bioinformatics, University of Pavia, Pavia, Italy
[c] CNR-ITB, Segrate, Milan, Italy
[d] Clinical Oncology Department, Fondazione IRCCS Policlinico San Matteo, Pavia, Italy
[e] Department of Biochemistry, University of Pavia, Pavia, Italy
[f] Clinical Chemistry Laboratories, Fondazione IRCCS Policlinico San Matteo, Pavia, Italy

ARTICLE INFO

Article history:
Received 10 November 2010
Received in revised form 23 December 2010
Accepted 28 December 2010
Available online 4 January 2011

Keywords:
Immunoglobulin free light chains
Amyloidosis
Immunoprecipitation
Proteomics
Post-translational modifications

ABSTRACT

An excess of circulating monoclonal free immunoglobulin light chains (FLC) is common in plasma cell disorders. A subset of FLC, as amyloidogenic ones, possess intrinsic pathogenicity. Because of their complex purification, little is known on the biochemical features of serum FLC, possibly related to their pathogenic spectrum. We developed an immunopurification approach to isolate serum FLC from patients with monoclonal gammopathies, followed by proteomic characterization. Serum monoclonal FLC were detected and quantified by immunofixation and immunonephelometry. Immunoprecipitation was performed by serum incubation with agarose beads covalently linked to polyclonal anti-κ or λ FLC antibodies. Isolated FLC were analyzed by SDS-PAGE, 2D-PAGE, immunoblotting, mass spectrometry (MS). Serum FLC were immunoprecipitated from 15 patients with ALλ amyloidosis (serum λ FLC range: 98–2350 mg/L), 5 with ALκ amyloidosis and 1 with κ light chain (LC) myeloma (κ FLC range: 266–2660 mg/L), and 3 controls. Monoclonal FLC were the prevalent eluted species in patients. On 2D-PAGE, both λ and κ FLC originated discrete spots with multiple *pI* isoforms. The nature of eluted FLC and coincidence with the LC sequence from the bone marrow clone was confirmed by MS, which also detected post-translational modifications, including truncation, tryptophan oxidation, cysteinylation, peptide dimerization. Serum FLC were purified in soluble form and adequate amounts for proteomics, which allowed studying primary sequence and detecting post-translational modifications. This method is a novel instrument for studying the molecular bases of FLC pathogenicity, allowing for the first time the punctual biochemical description of the circulating forms.

1. Introduction

An excess of circulating monoclonal free immunoglobulin light chains (FLC) is a common feature of many plasma cell disorders [1]. Besides being biomarkers of the bone marrow clone, a subset of monoclonal FLC possess intrinsic pathogenicity, becoming causative agents of diseases such as light chain (AL) amyloidosis or light chain deposition disease [2,3], and myeloma cast nephropathy. In AL amyloidosis, monoclonal FLC, transported to target organs through the bloodstream, lose their native conformation and aggregate into toxic species, causing severe tissue dysfunction. The molecular mechanisms behind the spectrum of pathogenic properties are likely to be related to peculiar biochemical features of FLC [2–5]. Most of the available knowledge on the characteristics of FLC has been derived from Bence Jones proteins or species extracted from amyloid deposits [5–8]. However, the properties of FLC from these sources may not coincide with those of the circulating ones, which are, instead, scarcely known due to the complexity of their isolation from blood. The major obstacles in this task are related to their usually low concentration compared to intact antibodies, and to the shared epitopes between bound and free light chains (LC), which prevent the purification of the unbound fraction with most high-affinity

Abbreviations: FLC, free light chains; LC, light chains; IEF, isoelectrofocusing; 2D-PAGE, two-dimensional polyacrylamide gel electrophoresis; MS, mass spectrometry; MALDI-TOF, matrix assisted laser desorption/ionization time of flight; PMF, peptide mass fingerprinting; DTT, dithiothreitol; LC-MS/MS, liquid chromatography tandem mass spectrometry; 2DC, two-dimensional chromatography

* Corresponding author. Centro per lo Studio e la Cura delle Amiloidosi Sistemiche, Fondazione IRCCS Policlinico San Matteo and University of Pavia, Viale Golgi 19, 27100 Pavia, Italy. Tel.: +39 0382 502994; fax: +39 0382 502990.
E-mail address: gmerlini@unipv.it (G. Merlini).

1570-9639/$ – see front matter © 2011 Elsevier B.V. All rights reserved.
doi:10.1016/j.bbapap.2010.12.012

commercial antibodies. Micromethods for serum FLC isolation, based on gel electrophoresis, have been described [9,10]. However, FLC purification in soluble form would increase the spectrum of potential analyses and in vitro applications to investigate their biological properties.

The exposure of epitopes hidden in the bound counterparts has been exploited to generate specific anti-FLC antibodies, employed in a commercial immunonephelometric assay [11]. We utilized these antibodies for developing an immunoprecipitation-based approach, to isolate FLC from serum of patients with monoclonal gammopathies. The purified FLC were subjected to proteomic analyses, which allowed to investigate amino acid sequence, charge properties and, for the first time, location of disulphide bridges and presence of selected post-translational modifications.

2. Methods

2.1. Patients and samples

Samples were obtained from patients referred to the Amyloid Treatment and Research Center in Pavia, Italy, upon acquisition of informed consent. Serum was obtained by centrifugation (4000 rpm, 10 min) of whole blood without anticoagulants. Monoclonal components were detected by high-resolution agarose gel electrophoresis/immunofixation, performed as described [12], and by the κ/λ ratio of serum FLC concentrations, measured by particle enhanced nephelometry (Freelite assay™, The Binding Site, Birmingham, UK), on a Behring BNII Nephelometer (Dade Behring, Deerfield, IL, USA) [11]. Upper reference limits for serum FLC concentrations are, respectively, 19.4 mg/L for κ and 26.3 mg/L for λ (normal κ/λ ratio interval 0.26–1.65). Samples were immediately additioned of protease inhibitors (Complete™, Roche, Basel, Switzerland) and frozen at -80 °C. The diagnosis of AL amyloidosis required the presence of Congo red birefringent amyloid fibrils in subcutaneous abdominal fat aspirates or organ biopsy, recognized by anti-LC antibodies by immuno-electron microscopy, along with evidence of a plasma cell dyscrasia. Sera from individuals with no evidence of monoclonal components and FLC excess served as controls.

2.2. Immunoaffinity purification of serum FLC

Sheep polyclonal antibodies anti-human free κ and λ LC were provided by The Binding Site. Surface-derivatized agarose beads (Aminolink Plus™) were from Pierce (Rockford, IL, USA). Anti-FLC antibodies were dialyzed against PBS, followed by covalent linkage to beads as indicated by Pierce (6.5 mg anti-λ FLC/mL beads; 9 mg anti-κ FLC/mL beads). After coupling, unbound antibodies were removed and the uncoupled reactive sites on the beads blocked. Coupling efficiency was estimated by the differential spectrophotometric absorbance at 280 nm of the antibody solution before and after incubation. Aliquots of coupled beads were placed in microcentrifuge spin columns (Pierce) (100 μg/column), each used for FLC immunoprecipitation from a single individual. Thawed serum samples were diluted 1:6 (1:2 for AL κ patients with serum κ FLC <300 mg/L; these dilutions were adopted due to the optimal visually estimated qualitative relation between captured FLC and background co-eluted proteins) in immunoprecipitation buffer (PBS/0.1% v/v Triton X-100; final volume per tube: 500 μL, corresponding to ~83 μL of serum), and incubated with coupled beads overnight at 4 °C, with end-over-end mixing. Unbound serum was removed by low-speed centrifugation, followed by extensive bead washing with PBS/0.1% v/v Triton X-100 and then with PBS alone. Elution of captured species was performed using 0.2 M glycine–HCl solution, pH 2.8 (3 mL/mg beads), followed by pH neutralization. Protein concentrations were measured using a bicinchoninic acid assay (Pierce). Eluates were aliquoted and stored at -80 °C until further analyses.

2.3. cDNA sequencing of monoclonal FLC

Total RNA was extracted from bone marrow mononuclear cells. Monoclonal LC variable regions were cloned by a universal inverse-PCR strategy [13]. After sequencing, standard RT-PCR was employed, using 5′ primers specific for each monoclonal VL (from codon +1 to +7), and a 3′ primer corresponding to the carboxy-terminal region of κ (Cκ primer: from codon +208 to +215, 5′-ACACTCTCCCCTGTT-GAAGCT-3′) or λ light chains (Cλ primer: from codon +208 to +215, 5′-TGAACATTCTGTAGGGGCCACTG-3′), in order to obtain the original full-length monoclonal LC sequence. The PCR-fragment was ligated into a cloning vector and cloned. After purification of recombinant plasmids, inserts were sequenced. To determine the presumed germline genes of Vλ/κ regions, sequence alignment was made with the current releases of EMBL-GenBank, V-BASE (V BASE Sequence Directory, MRC Centre for Protein Engineering, Cambridge, UK) and IMGT sequence directories. Theoretical molecular weight (MW) and isoelectric point (pI) were calculated using a dedicated tool available on the Expasy proteomic server website (www.expasy.org).

2.4. Gel electrophoresis

SDS-PAGE was performed under reducing (addition of β-mercaptoethanol) and non-reducing conditions according to Laemmli [14]. For 2D-PAGE analysis, the eluates from ~65 μL of serum were dialyzed against ultrapure water (18 h, 4 °C) and diluted in isoelectrofocusing (IEF) buffer (7 M urea, 2 M thiourea, 4% v/v CHAPS, 65 mM dithiothreitol (DTT)). First and second electrophoretic dimensions were conducted as described [8], using, respectively, 17 cm strips, non-linear 3–10 pH gradient (BioRad, Hercules, CA, USA) and 8–16% polyacrylamide gradient large format gels (BioRad). Proteins were reduced and alkylated between first and second dimension. All gels were stained with colloidal Coomassie blue (Pierce) and imaged using a VersaDoc instrument (BioRad). For Western blotting, separated proteins were transferred onto a PVDF membrane (GE Healthcare, Piscataway, NJ, USA) and probed with polyclonal rabbit anti-human κ or λ LC (Dako, Glostrup, Denmark; dilutions, respectively, 1:25,000 and 1:15,000), followed by incubation with an horseradish-peroxidase conjugated swine anti-rabbit secondary antibody.

2.5. Protein analysis by matrix-assisted laser desorption/ionization-time of flight (MALDI-TOF) MS

Protein spot excision and in-gel digestion were performed as previously described [8]. Briefly, the protein spots were destained, washed and digested with sequencing grade modified trypsin (Trypsin Gold, Promega, Madison, WI, USA). Peptides were extracted and prepared for MS using micro-reversed-phase chromatography (ZipTips™, Millipore, Billerica, MA, USA). Mass spectra were obtained after peptide co-crystallization with the α-cyano-hydroxycinnamic acid matrix onto target plates, using a Waters Micromass MicroMX MALDI-TOF MS instrument (Waters, Milford, MA, USA), operated in the positive ion, reflectron mode, over the *m/z* range 600–4000. External calibration was achieved using Waters ADH standard digestion mix, and internal calibration using Glu-Fibrinopeptide B as lock mass. Mass spectra were analyzed using MassLynx software (Waters). Deisotoped peak lists were submitted to the database search engine Mascot™ (Matrix Science, London, UK) for peptide mass fingerprinting (PMF) against the National Center for Biotechnical Information (NCBI) non-redundant protein database using the following restrictions: (a) Homo sapiens, (b) trypsin digestion, up to 2 missed cleavages, (c) 50-ppm error, (d) cysteine carbamidomethylation as fixed modification. For the database search settings reported, a

MOWSE score >66 was determined to yield a $p<0.05$ for false positive assignments. Peak assignments were also performed manually using theoretical digest values from bone marrow-deduced monoclonal LC sequences, with the online software tool MS-Digest (Protein Prospector, University of California, San Francisco, CA, USA).

2.6. Protein analysis by liquid chromatography mass spectrometry (LC-MS)

Eluates from ~65 μL of serum were concentrated 10-fold in a vacuum centrifuge, then dialyzed against 50 mM ammonium bicarbonate pH 8.8 (18 h, 4 °C). Protein reduction/alkylation was performed as follows: addition of DTT (final concentration 10 mM, 5 min at 95 °C, then 45 min at 25 °C); addition of iodoacetamide (final concentration 40 mM; 1 h at 25 °C); addition of DTT (final concentration 40 mM; 1 h at 25 °C). Proteins were digested with sequencing grade trypsin (Promega) (enzyme:substrate ratio 1:20 w/w) for 2 h at 37 °C, followed by a second step of digestion under the same conditions. The reaction was stopped by adding trifluoroacetic acid to a concentration of 1% v/v. Digested samples were analyzed by two-dimensional micro-liquid chromatography coupled to tandem mass spectrometry (2DC-MS/MS, also known as Multidimensional Protein Identification Technology, MudPIT) [15,16], using the Proteome X-2 system (Thermo Fisher, San José, CA, USA). Briefly, 10 μL of the peptide mixtures, previously diluted 1:2, were loaded onto a strong cation exchange column (Biobasic-SCX column, 0.32 i.d. × 100 mm, 5 μm, Thermo Scientific, Bellefonte, PA, USA) and then eluted stepwise by a four step ammonium chloride concentration gradient (0, 100, 400, 700 mM). Each salt step eluate was directly loaded onto a reversed-phase C18 column (Biobasic-18, 0.180 i.d. × 100 mm, 5 μm, Thermo Scientific, Bellefonte, PA, USA) and separated by an acetonitrile gradient (eluent A, 0.1% formic acid in water; eluent B, 0.1% formic acid in acetonitrile); the gradient profile was 5% eluent B for 5 min, 5–40% B in 45 min, 40–80% B in 10 min and 80–95% B in 10 min; flow-rate 1 μl/min. The peptides eluted from the C18 column were directly analyzed with an ion trap LTQ Orbitrap (Thermo Fisher, San Josè, CA, USA). Spectra were acquired in positive ion mode by acquiring a full MS scan in the range 400–2000 *m/z*, followed by four MS/MS scan of the four most intense ions, with 1 min dynamic exclusion. Using SEQUEST algorithm (University of Washington, licensed to Thermo Finnigan), the experimental mass spectra were correlated to the theoretical ones obtained by in silico digestion of a home-made subset database of immunoglobulin LC sequences (100 entries), downloaded from NCBI (www.ncbi.nlm.nih.gov) and UniProt (www.uniprot.org) databases. A database containing all the available bone marrow-derived FLC sequences of patients included in this study was also generated. Data processing was performed using the following parameters: no enzyme specificity; mass tolerance of 2.00 amu for peptide and 1.00 amu for MS/MS ions; minimum Xcorr values greater than 1.5, 2.0 and 2.5 respectively for single, double and triple charge ions during peptide matching; peptide/protein probability $<1\times10^{-3}$, consensus score >10. For protein identification, only the first-best matching peptide was taken into consideration and only if the same peptide was found in multiple MS/MS spectra. Selected post-translational modifications (tryptophan, cysteine and tyrosine oxidations, conversion of N-terminal glutamine to pyroglutamic acid, cysteinylation, presence of intra- or inter-chain disulphide-linked peptides) were investigated. The false discovery rate (FDR), obtained by processing the mass spectra using the reverse database of bone marrow-derived FLC sequences, was <5%.

3. Results

Serum FLC immunoprecipitation was performed from 15 unselected patients with serum monoclonal λ FLC, all affected by AL λ amyloidosis (serum λ FLC concentration range, measured by nephelometry: 98–2350 mg/L; κ/λ ratio range: 0.005–0.085), and from 6 unselected patients with κ monoclonal FLC (5 with AL κ

Table 1
Clinical and laboratory characteristics of patients with monoclonal gammopathies and controls included in the study.

Patient code	Gender, age	Diagnosis	Amyloid organ involvement [a]	Serum involved FLC (mg/L) (κ/λ ratio)	Monoclonal component at serum HRAGE-IFE [b]	Vλ or Vκ monoclonal FLC germline gene	Deduced MW/*pI* of cloned LC	Total proteins immunoprecipitated from 83 μL serum (μg)
ALλ 1	M, 56	MM + AL λ	ST, GI	1140 (0.007)	λ FLC	n.a.		29
ALλ 2	F, 71	MM + AL λ	H, K, ST	733 (0.048)	λ FLC	*IGLV3-1*	22.77 kDa/ 5.15	26
ALλ 3	M, 71	MM + AL λ	H, K, ST	1970 (0.007)	λ FLC	*IGLV3-25*	22.54 kDa/ 5.01	22
ALλ 4	M, 56	AL λ	H, GI	1050 (0.012)	IgGκ + λ FLC	*IGLV1-36*	22.7 kDa/5.15	22
ALλ 5	M, 73	AL λ	H, K, ST	2350 (0.005)	λ FLC	*IGLV3-21*	22.5 kDa/5.69	28
ALλ 6	M, 69	AL λ	H, PNS	429 (0.028)	IgG λ + λ FLC	*IGLV2-14*	22.8 kDa/7.05	18
ALλ 7	F, 69	WM + AL λ	K	228 (0.081)	IgM λ + λ FLC	n.a.		54
ALλ 8	M, 57	MM + AL λ	H	132 (0.075)	λ FLC	n.a.		21
ALλ 9	F, 45	MM + AL λ	K	98 (0.014)	IgG λ + λ FLC	n.a.		19
ALλ 10	F, 72	AL λ	H, K, PNS	248 (0.052)	λ FLC	*IGLV1-51*	22.7 kDa/8.55	25
ALλ 11	F, 49	AL λ	H, K, L	101 (0.085)	IgA λ + λ FLC	n.a.		23
ALλ 12	M, 65	AL λ	H	695 (0.076)	λ FLC	n.a.		23
ALλ 13	M, 69	AL λ	H	1070 (0.018)	λ FLC	n.a.		22
ALλ 14	M, 74	AL λ	H, K, PNS	1140 (0.01)	IgG λ + λ FLC	n.a.		23
ALλ 15	M, 45	AL λ	H	477 (0.017)	λ FLC	*IGLV1-51*	22.3/6.15	18
Ctrl λ 1	F, 49	Control λ		κ 12.8; λ 10.1 (1.26)	None			7.5
Ctrl λ 2	M, 37	Control λ		κ 13.5; λ 12.5 (1.08)	None			8
ALκ 1	M, 73	MM + AL κ	H	1160 (120.3)	IgAλ + K FLC	n.a.		9
MMκ 2	M, 49	MM + cast nephropathy		1710 (117.9)	K FLC	n.a.		13
ALκ 3	F, 63	AL κ	H, K, L	2660 (155.5)	K FLC	n.a.		14
ALκ 4	M, 54	MM + AL κ	K	1420 (845.2)	K FLC	n.a.		21
ALκ 5	M, 79	MM + AL κ	H, PNS, ST	266 (22.3)	IgG K + K FLC	n.a.		7
ALκ 6	M, 66	AL κ	H, GI, ST, K	1350 (73.3)	K FLC	*IGKV4-1*	24 kDa/6.48	19
Ctrl κ 1	F, 49	Control κ		κ 12.8; λ 10.1 (1.26)	None			2.5

Abbreviations: ST, soft tissues; GI, gastrointestinal tract; H, heart; K, kidney; PNS, peripheral nervous system; L, liver; MC, monoclonal component; MM, multiple myeloma; WM, Waldentrom's macroglobulinemia; HRAGE-IFE, high-resolution agarose gel electrophoresis and immunofixation; MW, molecular weight; *pI*, isoelectric point; n.a., not available.
[a] Defined according to the International Consensus Panel criteria (Gertz MA et al., Am. J. Hematol., 2005;79:319–28).
[b] See Supplemental Figures 1 and 2.

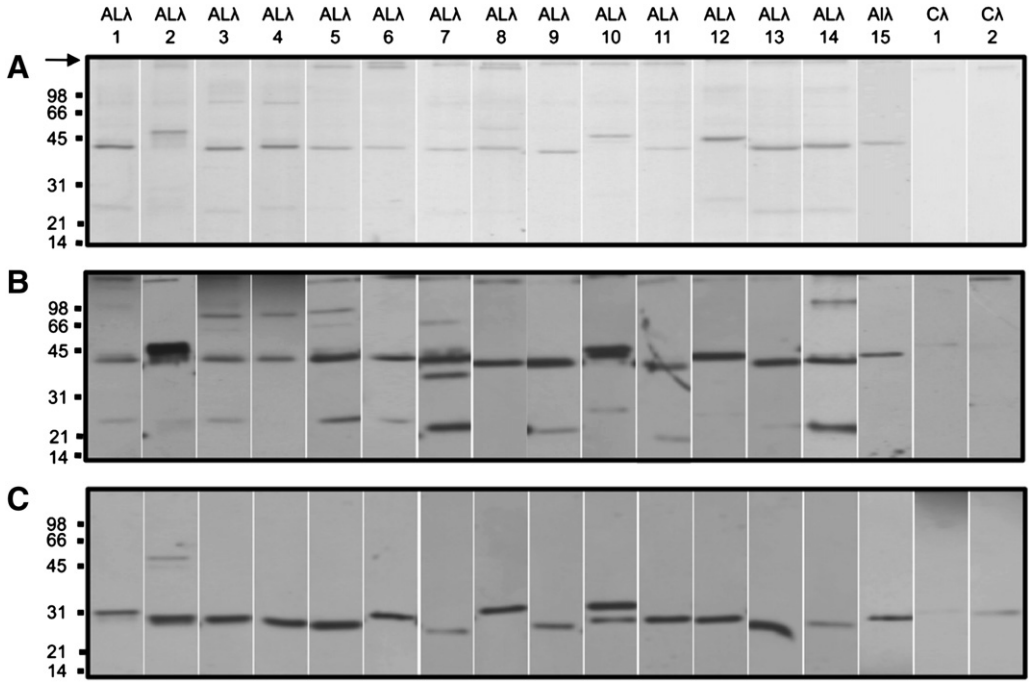

Fig. 1. Immunoprecipitated λ FLC after serum incubation with beads coupled to anti-human λ FLC antibodies in 15 patients with AL λ amyloidosis and 2 controls. (A) SDS-PAGE separation of eluted proteins, non-reducing conditions (Coomassie stain; the volume of eluate loaded for each patient was 1/16 of the total from ~83 μL of serum, equivalent to that from ~5 μL of serum). (B) Immunoblot, corresponding to the gel in (A), under non-reducing conditions, using anti-human λ LC primary antibodies. (C) Immunoblot of the same samples, separated under reducing conditions. High MW bands possibly corresponding to traces of intact immunoglobulins are indicated by an arrow.

amyloidosis and one with κ LC myeloma) (serum κ FLC range: 266–2660 mg/L; κ/λ ratio range: 22.3–845.2). This series of patients presented a wide range of circulating free light chain concentrations and heterogeneous serum protein electrophoretic patterns, including complete monoclonal immunoglobulins (Table 1 and Supplemental 1 and 2). Immunoprecipitations were also performed from control sera, to assess polyclonal LC background (one using anti-κ FLC and two using anti-λ FLC-coupled beads).

The quality of the immunoprecipitates was evaluated by multiple means, as described below (Figs. 1–3). In all patients, FLC were the prominent detectable eluted species. Using comparable quantities of coupled antibody and considering similar serum FLC concentrations, the total amount of precipitated proteins was generally higher for λ than κ cases (Table 1). We did not observe a linear relation between total eluted proteins and serum FLC concentration, possibly due to saturation of the system. Notably, FLC isolation was successful also in cases in which monoclonal free light chains appeared as faint bands at immunofixation (e.g., patients 8 and 10 in Supplemental Figure 1). The deduced aminoacid sequence of the monoclonal LC produced by the bone marrow clone was available in seven patients with AL λ amyloidosis and one with AL κ amyloidosis (Table 1).

3.1. Lambda FLC

Upon non-reducing SDS-PAGE, ~45 kDa λ FLC bands were the most intense visible species in the molecular weight range 14–100 kDa, along with minor ~22–25 kDa λ FLC bands (the identity of both was assessed by immunoblotting) (Fig. 1). These two bands collapsed into a single one upon reduction, confirming the nature of the higher MW one as the disulphide-linked FLC dimer. The electrophoretic mobility of the immunopurified λ FLC on the gels differed slightly between patients. Lambda FLC monomers and dimers originated single, discrete bands in all samples except in patients ALλ7 and ALλ10, in which minor associated immunoreactive bands were observed. The dimer stained more intensely than the monomer in all cases. In a subset of patients, additional immunoreactive species with a MW comprised between 45 and 100 kDa were visible, which disappeared upon sample reduction. Detectable but minimal levels of λ FLC were found in controls upon immunoblotting. The faint immunoreactive λ bands with highest MW (arrow in Fig. 1), visible in all non-reduced cases and controls, are compatible with traces of intact immunoglobulins.

The immunoprecipitates from five AL λ patients (ALλ 1–5) and one control (processed using anti-λ FLC antibodies) were analyzed by 2D-PAGE under reducing conditions (see representative maps in Fig. 3). Discrete prominent spots were visible in the ~25 kDa region of the gels in all patients (boxed) and not in the control. The migration pattern of these spots was peculiar for each patient.

Minor spots, not spatially associated to the previous ones, were also detectable, consistent with traces of other proteins. The absence of visible spots or smear consistent with light chain migration in the control confirms the low background of polyclonal FLC and intact immunoglobulins (which would dissociate into heavy and light chains upon reduction). In all patients, the ~25 kDa spots were excised, digested with trypsin and analyzed by MALDI-TOF MS (see representative patient ALλ5 in Fig. 4). The *m/z* values of the tryptic ion peaks visible in the spectra were compared with those derived from the in silico digestion of the bone marrow cloned light chains (available in patients ALλ 2-5). In all cases, the major peaks could be assigned to peptides from the respective monoclonal LC (see Fig. 4b); this allowed to assess the nature of the spots and to confirm clonality of the isolated species. Peptide ions from the LC variable regions were present in all patients' mass spectra. In two cases (ALλ2 and ALλ5), ions consistent with N-terminal peptides lacking the first aminoacid of the predicted LC sequence were observed. In patient ALλ5, this finding was confirmed by LC-MS/MS (see below). The *pI* distribution of the FLC spots was distinctive for each patient and was in accordance with the theoretical one, when available. Notably, all cases presented several detectable *pI* isoforms. The MALDI-TOF mass spectra from the various isoforms contained the same tryptic ion peaks belonging to the patients' monoclonal light chain; however, no clear differences in the spectra which could account for charge heterogeneity have been identified.

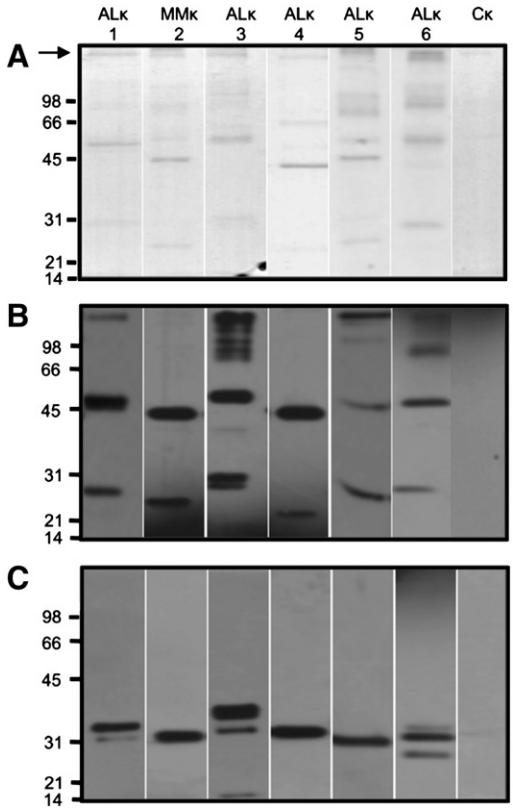

Fig. 2. Immunoprecipitated κ FLC after serum incubation with beads coupled to antihuman κ FLC antibodies in 5 patients with AL κ amyloidosis, 1 with κ micromolecular myeloma and 1 control. (A) SDS-PAGE separation of eluted proteins, non-reducing conditions (Coomassie stain). In patients ALκ1, MMκ2, ALκ3, ALκ4 and in the control, the loaded eluate was 1/16 of the total from ~83 μL of serum; in patients ALκ5, the loaded eluate was 1/16 of that obtained from ~166 μL of serum. (B) Immunoblot, using anti-human κ LC primary antibodies, under non-reducing conditions. (C) immunoblot of the same samples separated under reducing conditions. High MW bands possibly corresponding to traces of intact immunoglobulins are indicated by an arrow.

The major additional spots visible on the 2D gels were excised and identified by PMF (Fig. 3). Besides traces of albumin, faint spots constituted by clusterin (apolipoprotein J) were visible in all patients and in the control.

3.2. Kappa FLC

Upon non-reducing SDS-PAGE, two prominent bands, whose migration is consistent with the disulphide-linked κ LC dimer (~45–50 kDa) and monomer (~25–30 kDa) were visible in the 10–100 kDa MW region of gels (Fig. 2). Their nature as κ LC was confirmed by immunoblotting. The ~45 kDa bands are composed by disulphide-linked κ FLC dimers, as proved by their disappearance upon reduction. The apparent MW of the non-reduced monomers and dimers was on average slightly higher than what observed for λ FLC. The band corresponding to the κ LC dimer stained more or equally intensely than the monomer one in all cases. In patients ALκ1, ALκ3 and ALκ6, multiple anti-κ LC immunoreactive bands were visible in reduced samples. In patient ALκ3, a low MW (~15 kDa) κ band was evident, possibly corresponding to a fragment. Only traces of κ LC were visible in the control sample, under both reducing and non-reducing conditions. As observed in λ FLC, immunoreactive κ bands with a MW comprised between 50 and 100 kDa were visible in a subset of patients (ALκ3, ALκ 5 and ALκ6) in non-reduced samples. The highest MW κ bands (arrow in Fig. 2) are compatible with traces of intact immunoglobulins.

The eluates from patients ALκ4 and ALκ6 were analyzed by reducing 2D-PAGE (Figs. 3 and 5a, respectively), followed by MALDI-TOF MS analysis of the major visible spots. As in ALλ patients, discrete major trains of spots, migrating in a gel region corresponding to a MW of ~25 kDa, are visible in both patients (boxed). The trains consist of multiple *pI* isoforms of the patients' monoclonal LC, as confirmed by the presence of the same peaks in the MALDI-TOF mass spectra from the various spots (Fig. 5b). In patient ALκ4, where the bone marrow sequence was not available, the nature of the boxed spots as κ LC was confirmed by PMF search against NCBInr database (entry retrieved with highest significant score: NCBInr accession gi|5360679, MOWSE score 101; threshold 66). In patient ALκ6, the *m/z* values of the tryptic peptide ions matched those from the theoretical digest of the cloned LC sequence (Fig. 5b). In this patient, in accordance with what observed by reducing SDS-PAGE (Fig. 2), an additional species with lower apparent molecular weight (spot #4 in Fig. 5) was visible. The MALDI-TOF mass spectrum from this spot also contained tryptic ion peaks that could be assigned to the patient's monoclonal light chain. However, there was no clear evidence of missing peaks that could account for truncation and explain the lower MW. As shown in the spectra in Fig. 5, oxidation of peptides from the protein's variable region was detected. In particular, peaks consistent with different oxidation products of tryptophan 56 (hydroxytryptophan, +16 Da, N-formylkynurenine, +32 Da, and kynurenine, +4 Da) were visible (Fig. 5b). Minor spots corresponding to other proteins, mainly albumin and clusterin, were present.

3.3. 2DC-MS/MS analysis of the immunoprecipitated λ FLC

The immunoprecipitates from patients ALλ2, ALλ3, ALλ4, ALλ5 and ALλ15, whose cloned LC sequences were available, were analyzed by 2DC-MS/MS in non-reduced and reduced form. This allowed an extensive characterization of both constant and variable regions by direct sequencing of their primary structure (Fig. 6). While coverage of the constant region was high in all samples (ranging from 64% in patient ALλ15 to 84% in ALλ4; cumulative coverage 86%), that of the variable region varied (23% in ALλ2, 54% in ALλ3, 65% in ALλ4, 85.5% in ALλ5 and 42% in ALλ15). As shown, the contribution of non-tryptic peptides to the identification of the variable region was relevant, allowing to increase coverage. On the contrary, only few non-tryptic peptides were associated to the constant region. In patient ALλ5, LC-MS/MS confirmed the lack of the first N-terminal amino acid compared to the predicted sequence, also indicated by MALDI-TOF MS, suggesting possible N-terminal truncation.

3.4. Analysis of selected post-translational modifications

Oxidation of tryptophan residues was documented (Figs. 6 and 7a; Supplemental Fig. 3a–d). All aminoacid positions indicated in the text below refer to the LC sequences aligned as in Fig. 6. High-resolution analysis ($R = 60000$) and MS/MS spectrum sequencing allowed to identify three different oxidation products (hydroxytryptophan, N-formylkynurenine and hydroxyl-N-formylkynurenine) on W190 (constant region) of all samples and on W37 (variable region) of patient ALλ15. No oxidized tyrosine or cysteine residues were identified.

A dipeptide ($T_{135-154} + T_{195-209}$) due to the intra-chain disulphide bridge between cysteine residues in positions 139 and 198 (corresponding, respectively, to residues 134 and 194 according to the Kabat nomenclature) was identified in all samples (Figs. 7b and 8). This identification has been confirmed by the MS/MS fragmentation of the triple charged parent ion $[M + 3H^+]^{3+} = 1269.97\, m/z$. Oxidation on W153 within this dipeptide was also detected (Fig. 7b).

The contemporaneous presence, in non-reduced samples, of peptides containing S-cysteinylation on C198 (C194 according to Kabat nomenclature), was also documented in patients ALλ2, ALλ 3, ALλ 4 and ALλ 5 (Fig.6 and Supplemental Figure 4).

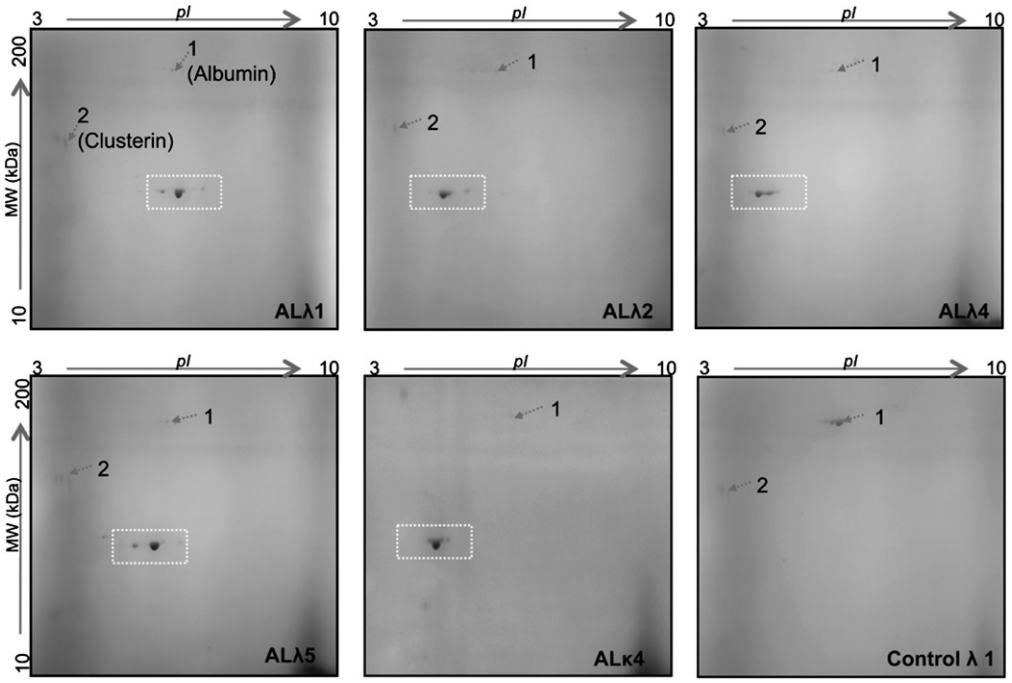

Fig. 3. 2D-PAGE separation (Coomassie stain) of immunoprecipitated proteins from 4 patients with AL λ amyloidosis, one with AL κ, and one control (whose serum was incubated with anti-λ FLC beads). The samples (80% of the total eluate from 83 μL of serum, equivalent to that from ~66 μL of serum) were separated on 3-10 non-linear pH gradient and 8-16% polyacrylamide gradient gels. Proteins were reduced and alkylated between first and second dimension. Major, closely associated spots visible in patients' gel regions corresponding to a MW of ~25 kDa are boxed. The boxed spots were excised, digested and analyzed by MALDI-TOF MS (see Figs. 4 and 5). The major other visible spots were also analyzed by MALDI-TOF MS and identified by PMF. Spots indicated as 1 and 2 are constituted by albumin (NCBInr accession gi|168988718, MOWSE score 226; threshold 66. Values refer to gel Control λ1, representative of the other experiments shown) and clusterin, respectively (NCBInr accession gi|178855, MOWSE score 138. Values refer to representative gel from Control λ 1).

```
  1 SYVLTQPHSV  SVAPGQTAKI  TCGGNNIGSE  SVHWYQQKPG  QAPVVVVYDD  SDRPSGIPER  FSGSNSGNTA  70
 71 TLTISRVGAG  DEADYYCQVW  DSSGDHGVFG  GGTKLTVLGQ  PKAAPSVTLF  PPSSEELQAN  KATLVCLISD  140
141 FYPGAVTVAW  KADSSPVKAG  VETTTPSKQS  NNKYAASSYL  SLTPEQWKSH  RSYSCQVTHE  GSTVEKTLAP  210
211 TECS                                                                              214
```

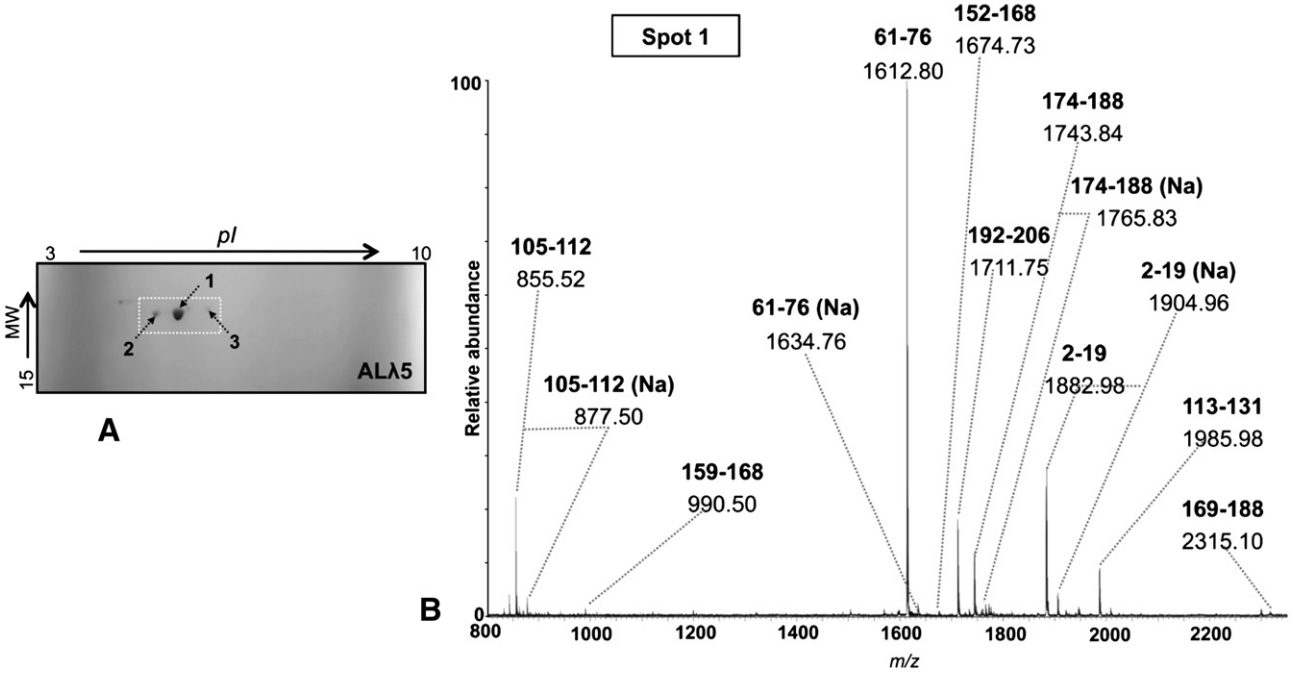

Fig. 4. MALDI-TOF MS analysis of immunoprecipitated λ FLC, separated by 2D-PAGE. (A) Detail of the 2D gel map from patient ALλ5, shown in Fig. 3. (B) MALDI-TOF MS spectrum from the tryptic digest of spot 1. The major peaks have been assigned to peptides from the theoretical digest of the patient's bone marrow-derived monoclonal LC sequence (shown above; sequence coverage is underlined). The *m/z* values and corresponding amino acid intervals (bold) in the LC sequence are shown above each peak. MALDI-TOF MS spectra from spots 1–3 contain the same ion peaks.

```
  1 DIVMTQSPDS LAVSLGERAT INCKSSQSAF YISNNKNYLA WYQQKPGQPP KLLISWASAR ESGVPDRFNG 70
 71 SGSGTDFTLT ISSLQAEDVA VYYCQHYFIT PVFGGGTKVE IKRTVAAPSV FIFPPSDEQL KSGTASVVCL 140
141 LNNFYPREAK VQWKVDHALQ SGNSQESVTE QDSKDSTYSL SSTPTLSKAD YEKHKVYACE VTHQGLSSPV 210
211 TKSFNRGEC                                                                  219
```

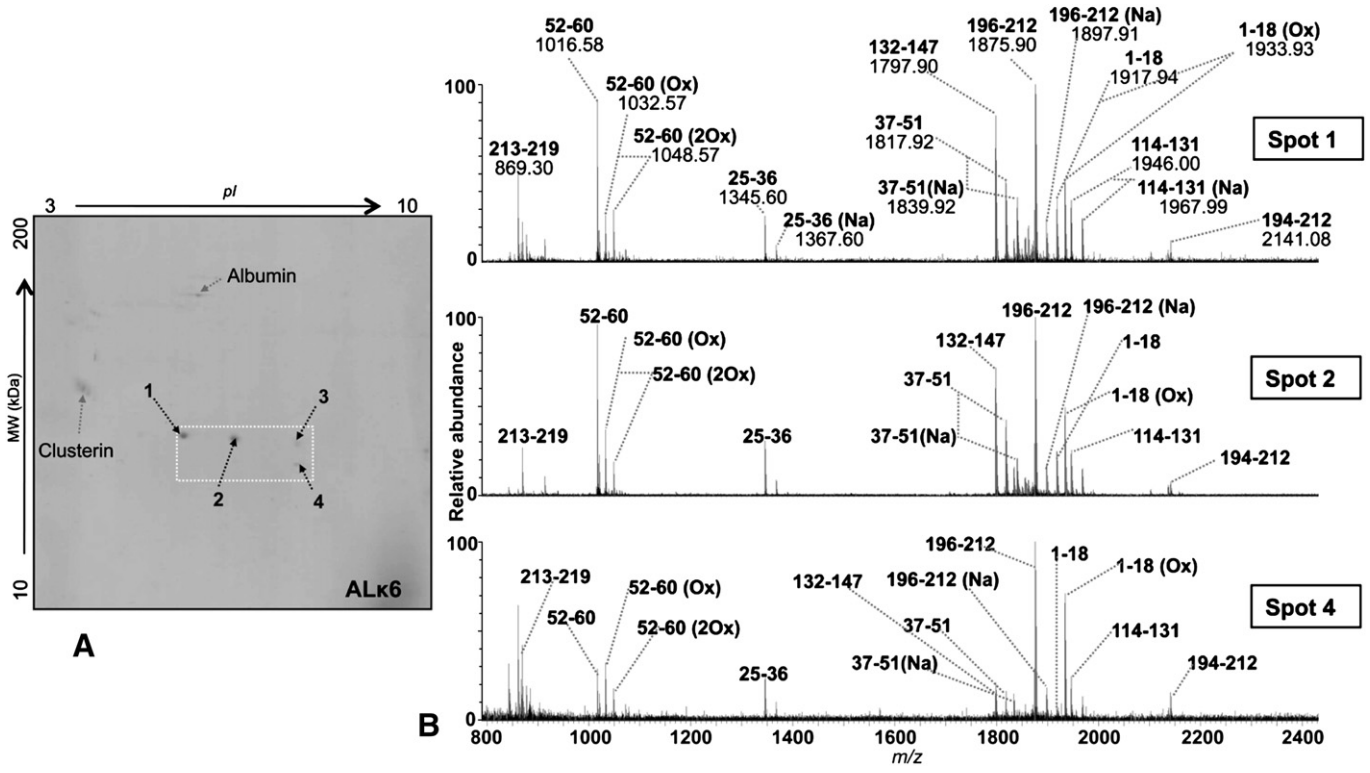

Fig. 5. 2D-PAGE separation and MALDI-TOF MS analysis of immunoprecipitated κ FLC in patient ALκ6. (A) 2D-PAGE map of immunoprecipitated proteins (80% of the total eluate from 83 μL of serum, equivalent to that from ~66 μL of serum) upon serum incubation with anti-human κ FLC, Coomassie stain. Spots in a gel region corresponding to aMWof ~25 kDa are boxed. (B) Overlayed MALDI-TOF MS spectra from tryptic digest of spots 1, 2 and 4. The major peaks have been assigned to peptides from the theoretical digest of the patient's bone marrow-derived monoclonal κ LC sequence (shown above; sequence coverage from spot 1 is underlined). The *m/z* values and corresponding aminoacid intervals (bold) in the LC sequence are shown above each peak. MALDI-TOF mass spectra from spots 1–4 contain the same tryptic ion peaks.

4. Discussion and conclusions

The method we describe allows to immunopurify FLC from serum in soluble form with a single-step procedure. The covalent immobilization of anti-FLC antibodies to beads avoids the drawbacks associated to traditional in-solution immunoprecipitation approaches, mostly based on retrieving the capture antibody by protein A or G, which would suffer from contamination of intact serum immunoglobulins, or on separation of the antibody–antigen complex by centrifugation, which requires antibodies with high avidity and may be inferior than bead-based methods in washing efficiency.

The described immunopurification is straightforward and requires little sample handling; moreover, performing immunoprecipitations in microcentrifuge spin columns with single-use beads allows optimal washing and avoids sample cross-contamination. Although varying between patients, amounts of immunoprecipitated FLC estimated to reach tens of micrograms were obtained from less than 100 μL of serum, with low levels of other serum proteins. The method has been tested over a wide range of serum FLC concentrations and could successfully isolate the antigen in all cases. This makes it a suitable tool for analyzing pathogenic FLC even when they circulate in low amounts, as is often the case in diseases such as AL amyloidosis [17]. Possibly due to intrinsic characteristics of the antibodies, the performance of the method at low FLC concentrations was better for λ than for κ light chains, in which a lower serum dilution had to be used during incubation.

The comprehensive biochemical characterization of circulating FLC was beyond the aim of this methodological work. However, the combined immunopurification/proteomic approach was efficient for their biochemical characterization, with unprecedented sensitivity and depth. Free light chains constitute an heterogeneous class of proteins, each one possessing unique chemical and biological properties due to the aminoacidic composition of the variable region [18,19]. The specificity in capturing the disease-related free light chains in this study was proved by 2D-PAGE and MS, which confirmed the concordance between the observed sequence and biochemical properties, and those predicted from the bone marrow clones.

FLC analysis under non-reducing conditions allows to investigate the extent of self-association by disulphide bridges. The prevalence of circulating λ disulphide-linked dimers over monomers is in accordance with what previously reported [20–22]. However, the same phenomenon was observed in isolated κ FLC, thought to circulate mostly as monomers [20]. The reason for this discrepancy is not clear, but we cannot exclude a preferential dimer recognition by antibodies in this application.

The nature of the high molecular weight immunoreactive bands observed upon non-reducing SDS-PAGE is unknown. Although the presence of light chain aggregates in vivo cannot be ruled out, their persistence in this setting would imply resistance to the strongly denaturing conditions used during the electrophoretic separation; the alternative hypothesis of their artifactual formation during analysis must be kept into account.

The LC epitopes recognized by the anti-free light chains antibodies are mostly located in the constant domain [1], allowing to capture FLC with different variable regions. However, although possible FLC fragments were observed in some of the cases described in our

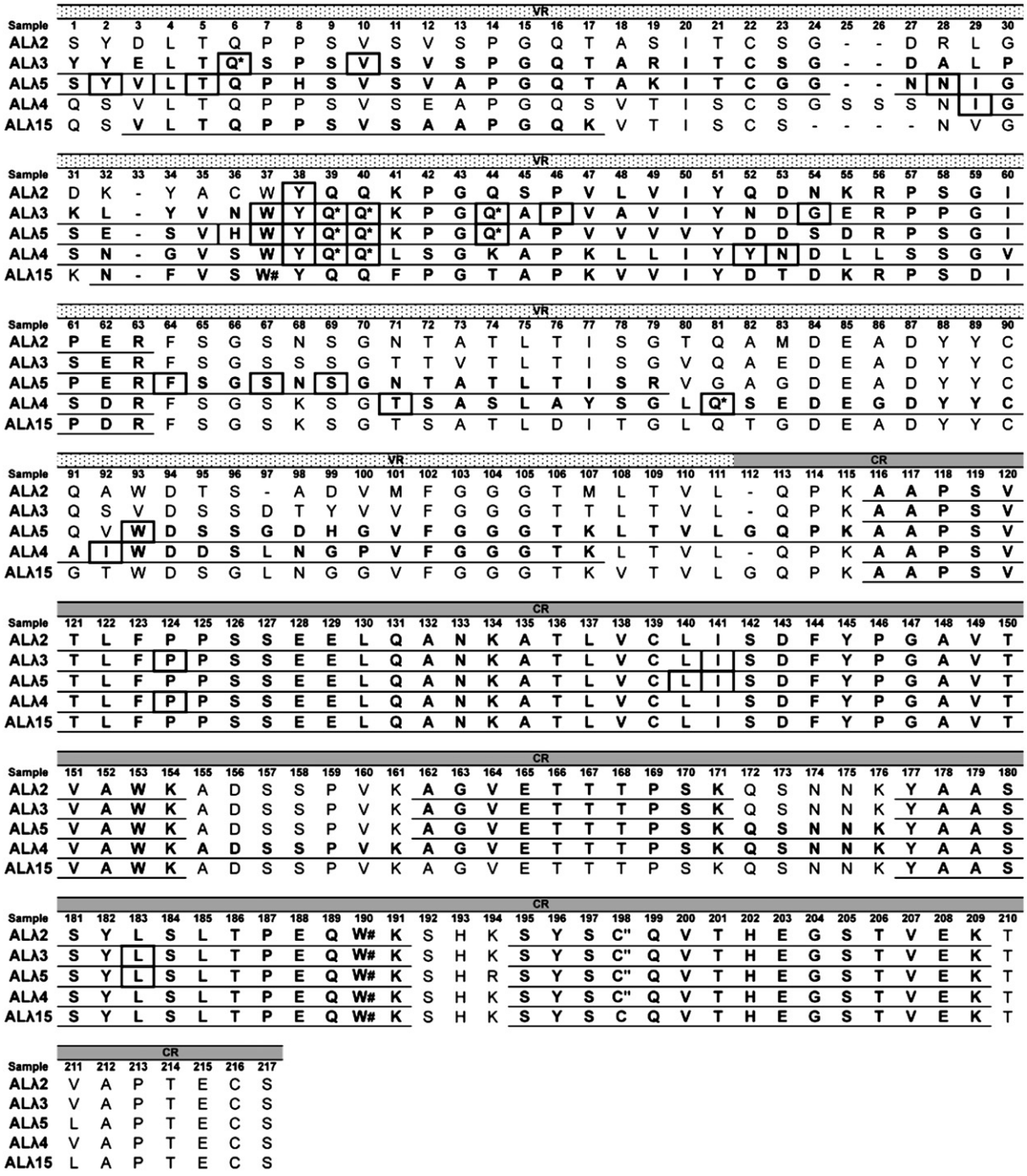

Fig. 6. Multiple sequence alignment, obtained by using the ClustalW tool (http://www.ebi.ac.uk/Tools/clustalw2/index.html), of 5 λ monoclonal FLC sequences deduced from bone marrow (CR: constant region; VR: variable region). The portions of sequences covered by peptides identified upon 2D-MS/MS are underlined. Variable regions were identified in the various FLC with an average of protein probabilities of 1×10^{-7} (protein probabilities ranging from 1×10^{-14} to 5×10^{-7}; threshold 1×10^{-3}), SEQUEST protein scores ranging from 30 to 168 (threshold: 10) and spectral count values ranging from 4 to 314. The constant regions were identified with an average of protein probabilities of 9×10^{-9} (protein probabilities ranging from 1×10^{-13} to 3×10^{-8}), SEQUEST protein scores ranging from 50 to 78 and spectral count values ranging from 24 to 88. The first aminoacid residue of non-tryptic peptides is included in rectangles. The modified aminoacid residues are highlighted in the figure: Q*6 in ALλ3; Q*39 and Q*40 in ALλ3, 4 and 5, Q*44 in ALλ3 and 5, Q*81 in ALλ4 correspond to N-terminal pyroQ (Δm = + 17 Da); W#190 in ALλ 2, 3, 4, 5 and 15 and W#37 in ALλ 15 correspond to three oxidation states of tryptophan (Hydroxy-tryptophan Δm = + 16 Da, N-formylkynurenine Δm = + 32 Da, Hydroxyl-N-formylkynurenine Δm = + 48 Da); C"198 in ALλ 2, 3, 4 and 5 correspond to S-cysteinylation (Δm = + 119 Da).

study, this method may not capture truncated forms constituted uniquely by the variable region, not bound by the antibodies [8,10].

There are several novel potentialities offered by the application of proteomics to the analysis of serum FLC. The available information about the biochemical features of ex-vivo pathogenic free light chains has so far been obtained from the investigation of Bence Jones proteins or light chains extracted from amyloid deposits. However, FLC from these sources are downstream "handling" products of the organism and may possess characteristics which do not reflect those of the circulating counterparts.

The proteomic search of signature biochemical features of subclasses of FLC with distinct biological properties, such as the amyloidogenic ones, is particular attractive. Our investigation of post-translational modifications of serum FLC is novel and allowed to unveil insofar unknown aspects of these proteins. Both 2D-PAGE coupled to MALDI-TOF MS and 2DC-MS/MS approaches revealed

heterogeneity within the populations of circulating FLC in all patients, with presence of multiple charge isoforms and N-terminal amino acid losses. The lack of the N-terminal aminoacid had been previously reported in a subset of Bence Jones proteins sequenced by Edman degradation (annotated in Kabat et al., Sequences of Proteins of Immunological Interest, 1991), supporting the validity of our finding in serum. Notably, 2D-PAGE had previously revealed the presence of multiple charge isoforms also in light chains extracted from amyloid deposits [8], and the comparison of the distribution of FLC from the two sources may provide hints on possible biochemical changes occurring during amyloidogenesis.

Oxidative post-translational modifications have been detected on the analyzed amyloidogenic serum FLC. Extensive and selective oxidation of specific tryptophan residues (such as W190 in Fig. 6), in particular, has been demonstrated in all cases. Its finding both in 2D-PAGE-separated FLC and upon MS analysis of in-solution digested proteins suggests that this modification is not exclusively linked to the sample processing method, and supports the hypothesis of a possible in vivo origin [23]. Although the time and site (before or after secretion from the plasma cell) of oxidation is still unknown, this modification may be related to increased oxidative stress, known to occur during amyloidoses [24,25]; moreover, it might play a role, among other factors, in destabilizing the protein structure [26,27].

An intriguing topic will be the investigation of cysteines in reduced and native states, to detect post-translational modifications and locate the residues involved in disulphide bridges. S-cysteinylation of the C-terminal cysteine of κ Bence Jones proteins has been previously reported [7]. However, the finding of partial S-cysteinylation of C194

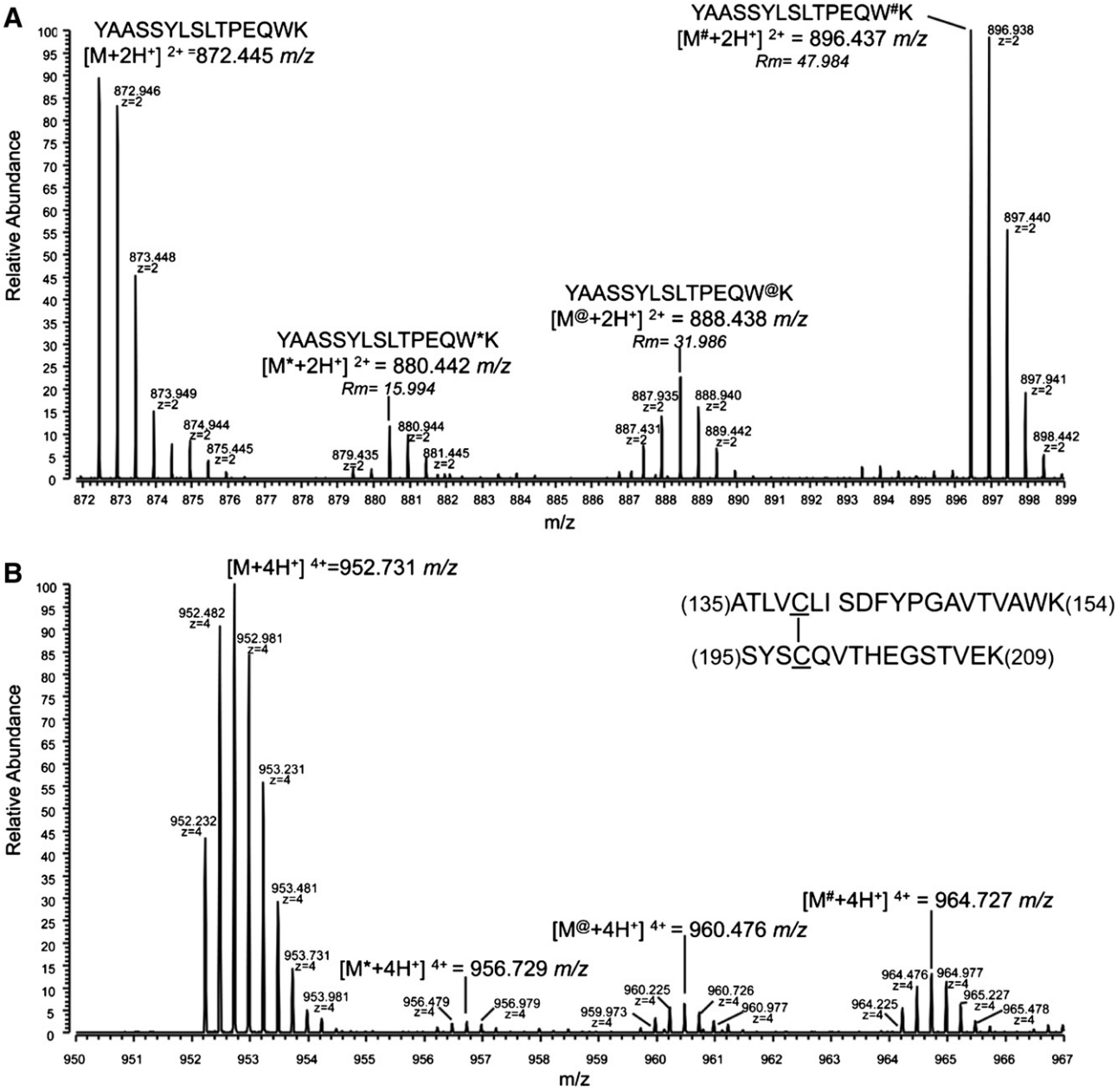

Fig. 7. (A) Oxidation states of the W190 in the tryptic unmodified peptide YAASSYLSLTPEQWK (parent ion $[M+2H^+]^{2+} = 872.445 m/z$) of the FLC constant region (patient ALλ5). MS spectrum from 872 to 899 m/z, acquired in high-resolution mode ($R = 60000$), is reported (C18 retention time = 35.81 min at 100 mM NH_4Cl mM salt step). Three different oxidation products are present: W* corresponds to hydroxy-tryptophan; W@ corresponds to N-formylkynurenine; W# corresponds to hydroxyl-N-formylkynurenine. Rm indicates the relative mass differences, due to different oxidation states, calculated respect to the double charged ion of the unmodified peptide.(B) MS spectrum from 950 to 970 m/z acquired in high-resolution mode ($R = 60000$) of the intra-chain double peptide ($T_{135-154} + T_{195-209}$) containing the disulphide bridge between C139 and C198 identified in all samples (amino acid positions refer to sequences aligned as in Fig. 6; see text for further details). Three different oxidation states have been observed on W153.

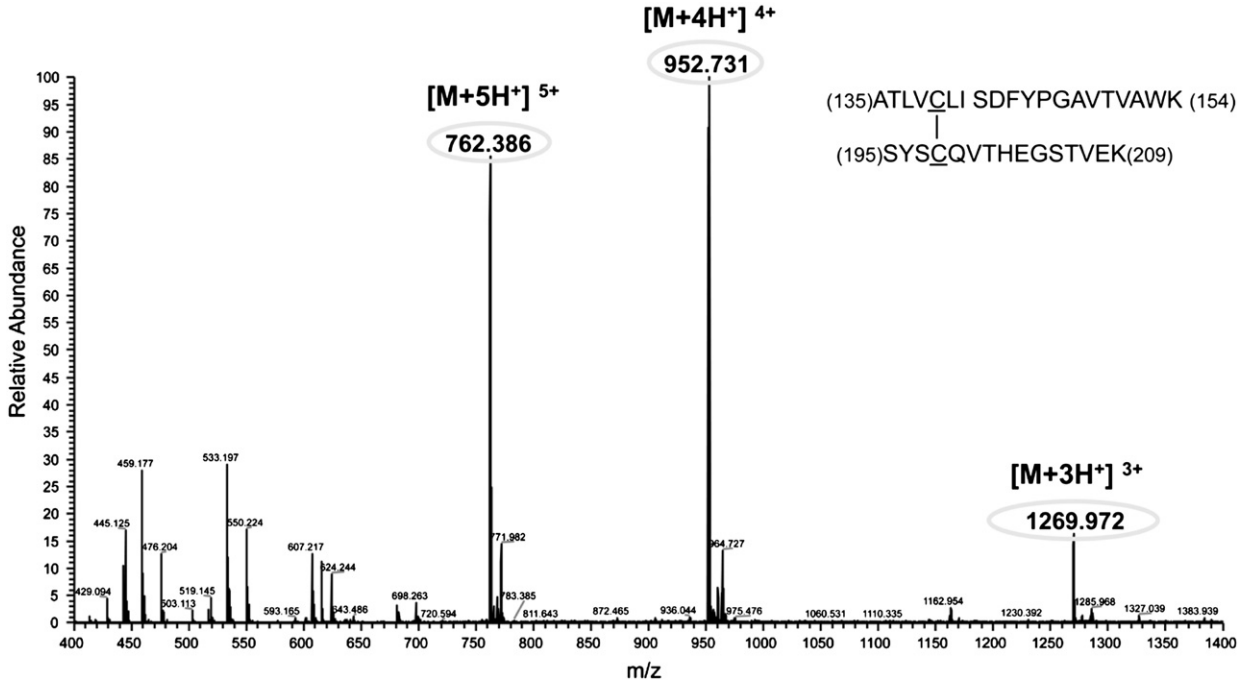

Fig. 8. Multi-charge MS spectrum of the dipeptide ($T_{135-154} + T_{195-209}$) identified as three to fivefold charged molecular ions ($[M + 3/5H^+]^{3/5+}$). See also Fig. 7b (amino acid positions refer to sequences aligned as in Fig. 6).

(according to Kabat nomenclature) in serum λ FLC, involved in the stabilizing intra-chain disulphide bridge within the constant region [28,29], was unexpected and suggests the existence of a rearrangement in the pattern of disulphide bonds in a fraction of circulating molecules.

Minor amounts of other serum proteins were found in the immunoprecipitates. Besides albumin, which was detectable only in traces, the only other spots visible in all cases by 2D-PAGE were constituted by clusterin (apolipoprotein J). Clusterin is involved in a variety of regulatory activities, is known to be a common constituent of amyloid deposits [30] and to interact with amyloidogenic proteins and various partners, among which immunoglobulins [31–33]. Although its finding in AL amyloidosis patients is intriguing, the presence also in the control sample may indicate its association with the bead-bound antibodies, which prevents its complete removal during washings. The targeted investigation of the co-immunoprecipitating species, however, may reveal the existence of an FLC interactome, disclosing protein partners involved in the biology of disorders such as monoclonal gammopathies and amyloidosis.

Another interesting application of LC-MS/MS analysis of serum FLC will be the chance to monitor the presence of specific and unique peptides from the patients' pathogenic chain, such as those from the variable region, to be used as biomarkers of the plasma cell clone. This may provide a novel and specific molecular tool for sorting the clone-produced LC over the polyclonal background, which could be of help, for example, in the non-invasive evaluation of residual disease after chemotherapy.

In conclusion, this study shows the feasibility of capture and proteomic analysis of serum FLC, and grants the extension and validation of the method on a wider population of individuals with characterized monoclonal gammopathies.

Supplementary materials related to this article can be found online at doi:10.1016/j.bbapap.2010.12.012.

Acknowledgments

We are grateful to Dr. Barbara Amoroso and Dr. Stephen Harding (The Binding Site) for providing the antibodies, and to Prof. Vittorio Bellotti for critically reviewing the manuscript and for his helpful suggestions. Support to this study was provided from the EURAMY project, which has received research funding from the Community's Sixth Framework Program, Fondazione Cariplo (Milano, Italy, N2009-2532), Ricerca Finalizzata Malattie Rare, Ministero della Salute, Istituto Superiore di Sanità (526D/63), and Ministry of Research and University (2007AESFX2_003).

References

[1] A. Dispenzieri, R. Kyle, G. Merlini, J.S. Miguel, H. Ludwig, R. Hajek, A. Palumbo, S. Jagannath, J. Blade, S. Lonial, M. Dimopoulos, R. Comenzo, H. Einsele, B. Barlogie, K. Anderson, M. Gertz, J.L. Harousseau, M. Attal, P. Tosi, P. Sonneveld, M. Boccadoro, G. Morgan, P. Richardson, O. Sezer, M.V. Mateos, M. Cavo, D. Joshua, I. Turesson, W. Chen, K. Shimizu, R. Powles, S.V. Rajkumar, B.G. Durie, International Myeloma Working Group guidelines for serum-free light chain analysis in multiple myeloma and related disorders, Leukemia 23 (2009) 215–224.
[2] G. Merlini, V. Bellotti, Molecular mechanisms of amyloidosis, N. Engl. J. Med. 349 (2003) 583–596.
[3] L. Obici, V. Perfetti, G. Palladini, R. Moratti, G. Merlini, Clinical aspects of systemic amyloid diseases, Biochim. Biophys. Acta 1753 (2005) 11–22.
[4] V. Bellotti, M. Nuvolone, S. Giorgetti, L. Obici, G. Palladini, P. Russo, F. Lavatelli, V. Perfetti, G. Merlini, The workings of the amyloid diseases, Ann. Med. 39 (2007) 200–207.
[5] V. Bellotti, P. Mangione, G. Merlini, Review: Immunoglobulin light chain amyloidosis—the archetype of structural and pathogenic variability, J. Struct. Biol. 130 (2000) 280–289.
[6] K.E. Olsen, K. Sletten, P. Westermark, Extended analysis of Al-amyloid protein from abdominal wall subcutaneous fat biopsy: kappa IV immunoglobulin light chain, Biochem. Biophys. Res. Commun. 245 (1998) 713–716.
[7] L.H. Connors, Y. Jiang, M. Budnik, R. Theberge, T. Prokaeva, K.L. Bodi, D.C. Seldin, C.E. Costello, M. Skinner, Heterogeneity in primary structure, post-translational modifications, and germline gene usage of nine full-length amyloidogenic kapp a1 immunoglobulin light chains, Biochemistry 46 (2007) 14259–14271.
[8] F. Lavatelli, D.H. Perlman, B. Spencer, T. Prokaeva, M.E. Mccomb, R. Theberge, L.H. Connors, V. Bellotti, D.C. Seldin, G. Merlini, M. Skinner, C.E. Costello, Amyloidogenic and associated proteins in systemic amyloidosis proteome of adipose tissue, Mol. Cell. Proteomics 7 (2008) 1570–1583.
[9] B. Kaplan, M. Ramirez-Alvarado, L. Sikkink, S. Golderman, A. Dispenzieri, A. Livneh, G. Gallo, Free light chains in plasma of patients with light chain amyloidosis and non-amyloid light chain deposition disease. High proportion and heterogeneity of disulfide-linked monoclonal free light chains as pathogenic features of amyloid disease, Br. J. Haematol. 144 (2009) 705–715.
[10] B. Kaplan, M. Ramirez-Alvarado, A. Dispenzieri, S.R. Zeldenrust, N. Leung, A. Livneh, G. Gallo, Isolation and biochemical characterization of plasma monoclonal free light chains in amyloidosis and multiple myeloma: a pilot study of intact and

truncated forms of light chains and their charge properties, Clin. Chem. Lab. Med. 46 (2008) 335–341.
[11] A.R. Bradwell, H.D. Carr-Smith, G.P. Mead, L.X. Tang, P.J. Showell, M.T. Drayson, R. Drew, Highly sensitive, automated immunoassay for immunoglobulin free light chains in serum and urine, Clin. Chem. 47 (2001) 673–680.
[12] G. Merlini, S. Marciano, C. Gasparro, I. Zorzoli, T. Bosoni, R. Moratti, The Pavia approach to clinical protein analysis, Clin. Chem. Lab. Med. 39 (2001) 1025–1028.
[13] V. Perfetti, M. Sassano, P. Ubbiali, M.C. Vignarelli, E. Arbustini, A. Corti, G. Merlini, Inverse polymerase chain reaction for cloning complete human immunoglobulin variable regions and leaders conserving the original sequence, Anal. Biochem. 239 (1996) 107–109.
[14] U.K. Laemmli, Cleavage of structural proteins during the assembly of the head of bacteriophage T4, Nature 227 (1970) 680–685.
[15] P. Mauri, A. Scarpa, A.C. Nascimbeni, L. Benazzi, E. Parmagnani, A. Mafficini, M. Della Peruta, C. Bassi, K. Miyazaki, C. Sorio, Identification of proteins released by pancreatic cancer cells by multidimensional protein identification technology: a strategy for identification of novel cancer markers, FASEB J. 19 (2005) 1125–1127.
[16] M.P. Washburn, D. Wolters, J.R. Yates III, Large-scale analysis of the yeast proteome by multidimensional protein identification technology, Nat. Biotechnol. 19 (2001) 242–247.
[17] G. Palladini, P. Russo, T. Bosoni, L. Verga, G. Sarais, F. Lavatelli, M. Nuvolone, L. Obici, S. Casarini, S. Donadei, R. Albertini, G. Righetti, M. Marini, M.S. Graziani, G.V. Melzi D'eril, R. Moratti, G. Merlini, Identification of amyloidogenic light chains requires the combination of serum-free light chain assay with immunofixation of serum and urine, Clin. Chem. 55 (2009) 499–504.
[18] A. Solomon, D.T. Weiss, Structural and functional properties of human lambda-light-chain variable-region subgroups, Clin. Diagn. Lab. Immunol. 2 (1995) 387–394.
[19] R.L. Comenzo, Y. Zhang, C. Martinez, K. Osman, G.A. Herrera, The tropism of organ involvement in primary systemic amyloidosis: contributions of Ig V(L) germ line gene use and clonal plasma cell burden, Blood 98 (2001) 714–720.
[20] K. Solling, Polymeric forms of free light chains in serum from normal individuals and from patients with renal diseases, Scand. J. Clin. Lab. Invest. 36 (1976) 447–452.
[21] K. Solling, Light chain polymerism in normal individuals in patients with severe proteinuria and in normals with inhibited tubular protein reabsorption by lysine, Scand. J. Clin. Lab. Invest. 40 (1980) 129–134.
[22] R.S. Abraham, M.C. Charlesworth, B.A. Owen, L.M. Benson, J.A. Katzmann, C.B. Reeder, R.A. Kyle, Trimolecular complexes of lambda light chain dimers in serum of a patient with multiple myeloma, Clin. Chem. 48 (2002) 1805–1811.
[23] I. Perdivara, L.J. Deterding, M. Przybylski and K.B. Tomer, Mass spectrometric identification of oxidative modifications of tryptophan residues in proteins: chemical artifact or post-translational modification?, J. Am. Soc. Mass. Spectrom. 21 1114-7.
[24] D.A. Brenner, M. Jain, D.R. Pimentel, B. Wang, L.H. Connors, M. Skinner, C.S. Apstein, R. Liao, Human amyloidogenic light chains directly impair cardiomyocyte function through an increase in cellular oxidant stress, Circ. Res. 94 (2004) 1008–1010.
[25] M.T. Lin, M.F. Beal, Mitochondrial dysfunction and oxidative stress in neurodegenerative diseases, Nature 443 (2006) 787–795.
[26] E.L. Finley, J. Dillon, R.K. Crouch, K.L. Schey, Identification of tryptophan oxidation products in bovine alpha-crystallin, Protein Sci. 7 (1998) 2391–2397.
[27] R. Rakhit, P. Cunningham, A. Furtos-Matei, S. Dahan, X.F. Qi, J.P. Crow, N.R. Cashman, L.H. Kondejewski, A. Chakrabartty, Oxidation-induced misfolding and aggregation of superoxide dismutase and its implications for amyotrophic lateral sclerosis, J. Biol. Chem. 277 (2002) 47551–47556.
[28] G.W. Litman, R.A. Good, D. Frommel, A. Rosenberg, Conformational significance of the intrachain disulfide linkages in immunoglobulins, Proc. Natl Acad. Sci. USA 67 (1970) 1085–1092.
[29] L.A. Steiner, Immunoglobulin disulfide bridges: theme and variations, Biosci. Rep. 5 (1985) 973–989.
[30] J.A. Vrana, J.D. Gamez, B.J. Madden, J.D. Theis, H.R. Bergen III, A. Dogan, Classification of amyloidosis by laser microdissection and mass spectrometry-based proteomic analysis in clinical biopsy specimens, Blood 114 (2009) 4957–4959.
[31] K.W. Lee, D.H. Lee, H. Son, Y.S. Kim, J.Y. Park, G.S. Roh, H.J. Kim, S.S. Kang, G.J. Cho, W.S. Choi, Clusterin regulates transthyretin amyloidosis, Biochem. Biophys. Res. Commun. 388 (2009) 256–260.
[32] M.R. Wilson, S.B. Easterbrook-Smith, Clusterin binds by a multivalent mechanism to the Fc and Fab regions of IgG, Biochim. Biophys. Acta 1159 (1992) 319–326.
[33] J.R. Kumita, S. Poon, G.L. Caddy, C.L. Hagan, M. Dumoulin, J.J. Yerbury, E.M. Stewart, C.V. Robinson, M.R. Wilson, C.M. Dobson, The extracellular chaperone clusterin potently inhibits human lysozyme amyloid formation by interacting with prefibrillar species, J. Mol. Biol. 369 (2007) 157–167.